CD45 alleviates airway inflammation and lung fibrosis by limiting expansion and activation of ILC2s

Guangwei Cui[a,1,2], Akihiro Shimba[a,b,1], Jianshi Jin[c,3], Nozomi Hojo[c] (ID), Takuma Asahi[a], Shinya Abe[a], Aki Ejima[a], Shinri Okada[a], Keizo Ohira[a], Ryoma Kato[a], Shizue Tani-ichi[a,b], Ryo Yamada[d] (ID), Takashi Ebihara[e] (ID), Katsuyuki Shiroguchi[c] (ID), and Koichi Ikuta[a,2]

Group 2 innate lymphoid cells (ILC2s) are critical for the immune response against parasite infection and tissue homeostasis and involved in the pathogenesis of allergy and inflammatory diseases. Although multiple molecules positively regulating ILC2 development and activation have been extensively investigated, the factors limiting their population size and response remain poorly studied. Here, we found that CD45, a membrane-bound tyrosine phosphatase essential for T cell development, negatively regulated ILC2s in a cell-intrinsic manner. ILC2s in CD45-deficient mice exhibited enhanced proliferation and maturation in the bone marrow and hyperactivated phenotypes in the lung with high glycolytic capacity. Furthermore, CD45 signaling suppressed the type 2 inflammatory response by lung ILC2s and alleviated airway inflammation and pulmonary fibrosis. Finally, the interaction with galectin-9 influenced CD45 signaling in ILC2s. These results demonstrate that CD45 is a cell-intrinsic negative regulator of ILC2s and prevents lung inflammation and fibrosis via ILC2s.

innate lymphoid cell | airway inflammation | fibrosis | CD45 | metabolism

Group 2 innate lymphoid cells (ILC2s) are critical for response against parasite infections and tissue homeostasis (1, 2). ILC2s are tissue-resident lymphocytes enriched in mucosal tissues such as the lung and intestine (3). GATA3, the master transcription factor of ILC2s and Th2 cells, is essential for ILC2s development and function (4). In addition, developing ILC2s express transcriptional factors such as Id2, TCF-1, RORα, and Gfi1, which are important for T cell differentiation (2, 5–7). In the adult bone marrow, ILC2s develop from common lymphoid progenitors (CLPs), followed by common helper-like ILC progenitors (CHILPs), and finally differentiate into ILC2 precursors (ILC2Ps) and mature ILC2s (mILC2s) (8).

Multiple molecules that positively control the development and activation of ILC2s have been investigated. First, ST2, a subunit of the IL-33R, is expressed by almost all tissue ILC2s. IL-33, a cytokine released from endothelial cells, epithelial cells, and preadipocytes, binds to ST2, promotes the proliferation of ILC2s, and elevates the production of type 2 cytokines such as IL-5 and IL-13 (1). Second, IL-17RB, a component of the IL-25R, is highly expressed on ILC2s in the intestine. Upon IL-25 stimulation, some ILC2s are activated and become inflammatory ILC2s, which produce IL-17 in addition to type 2 cytokines (9, 10). Third, ILC2s express cytokine receptors such as CD25 (IL-2Rα), CD127 (IL-7Rα), and thymic stromal lymphopoietin receptor (TSLPR), which transmit signals for the homeostasis and activation of ILC2s (2, 11–13). Finally, ILC2s express several costimulatory molecules critical for T cell immune response, such as inducible T cell costimulator (ICOS), tumor necrosis factor receptor 2 (TNFR2), and glucocorticoid-induced TNFR-related protein (GITR), which enhance the effector functions of ILC2s (14–16).

Although the population size of ILC2s is controlled in the steady state, ILC2s expand after activation and exert critical functions at the initiation and amplification phases of type 2 inflammation. Conversely, excessive inflammatory reactions of ILC2s trigger the pathogenesis of asthma, pulmonary fibrosis, and acute lung injury. Asthma is induced and exacerbated by the type 2 cytokines ILC2s and Th2 cells produce. IL-5 promotes eosinophil activation and recruitment to the lung, and IL-13 induces goblet cell hyperplasia and mucus production (17). ILC2s increase in number in asthma patients and exhibit activated phenotypes (18). Furthermore, type 2 immunity plays an essential role in idiopathic pulmonary fibrosis. The type 2 cytokines from ILC2s act on lung fibroblasts to elevate collagen production and promote fibrosis (19, 20). Thus, elucidating the regulatory mechanisms of ILC2s in the steady state and inflammation is vital to prevent and treat these respiratory diseases.

Several reports have shown that some molecules suppressing T cell activation, such as IFNR, IL-27R, and programmed cell death 1 (PD-1), are induced in ILC2s upon activation or maturation and suppress the activated ILC2s (21–23). Both type 1 and type 2

Significance

ILC2s trigger the pathogenesis of allergic airway inflammation and pulmonary fibrosis. However, the regulatory mechanism limiting ILC2 population size and inflammatory responses remain poorly studied. This study identified CD45 as a regulatory factor of ILC2s in the steady state and inflammations. ILC2s in the CD45-deficient mice exhibited enhanced proliferation and maturation in the bone marrow and hyperactivated phenotypes in the lung with elevated glycolytic metabolism. Functionally, CD45 signaling suppressed the lung ILC2s and was involved in the alleviation of airway inflammation and pulmonary fibrosis. Our study highlights that CD45 functions as a unique regulator of ILC2s for suppressing excessive type 2 inflammatory responses.

interferons and IL-27 suppress ILC2s through their receptors, which depends on STAT1 signaling (21). PD-1 inhibits ILC2 proliferation via metabolic regulation (22). Additionally, the aryl hydrocarbon receptor (AhR) inhibits the activation of gut-resident ILC2s (24). More recently, Regnase-1, an RNase critical for post-transcriptional control of mRNA, suppresses ILC2s by regulating *Gata3* and *ICOS* mRNA (25). However, whether there are common regulatory molecules suppressing ILC2s in the steady state and inflammation remains to be determined.

CD45 is a transmembrane tyrosine phosphatase and major cell surface glycoprotein exclusively expressed in all hematopoietic cells, including T cells and ILC2s. CD45-deficient mice and humans exhibit a profound T cell development block, resulting in severe combined immunodeficiency (26, 27). In addition, CD45 is critical in lymphocyte activation by dephosphorylating Src family kinases such as Lck, Fyn, and Lyn (28, 29). In T cells, CD45 dephosphorylates an activating tyrosine residue, Y394, and an inhibitory tyrosine residue, Y505, to control the activity of Lck (28). Furthermore, glycosylation of CD45 modulates the binding of natural ligands such as galectins, which alter the functions of CD45. For example, in thymocytes and activated T cells, a soluble lectin galectin-1 binds to CD45 and modulates cell death by regulating the clustering and phosphatase activity of CD45 (30). However, apart from its essential roles in T cell development and activation, the function of CD45 in ILC2s remains completely unknown.

To explore the function of CD45 in ILC2s, we analyzed a CD45-deficient mouse line. ILC2s in the CD45-deficient mice exhibited enhanced proliferation and maturation in the bone marrow and hyperactivated phenotypes in the lung with elevated glycolytic activity. Furthermore, CD45 signaling suppressed the type 2 inflammatory response by lung ILC2s and alleviated airway inflammation and pulmonary fibrosis. In addition, galectin-9 may interact with CD45 on ILC2s and modulate their effector functions. Thus, this study demonstrates that CD45 limits the expansion and activation of ILC2s and alleviates lung inflammation and fibrosis.

Results

CD45 Restrains Expansion, Maturation, and Cytokine Production of ILC2s. CD45 is remarkably expressed on the cell surface of T cells throughout their lifespan and plays an essential role in T cell development. Here, we found that ILC2s constantly expressed CD45 at comparable levels to T cells in the steady state (Fig. 1*A*). To investigate whether CD45 regulates the development and function of ILC2s, we employed a CD45-deficient (CD45$^{-/-}$) mouse line lacking exon 14 of the CD45 locus, in which the translation stopped within exon 15 before the transmembrane domain, and the expression of CD45 was utterly absent from cell surface (*SI Appendix,* Fig. S1 *A–C*). Furthermore, we confirmed that the mRNA expression on the 5′ side of exon 14 of CD45 is markedly decreased in cells, and the CD45 protein also disappeared from the cytoplasm of CD45$^{-/-}$ ILC2s (*SI Appendix,* Fig. S1 *D* and *E*). Given that CD45 deficiency significantly alters the cell numbers of primary lymphocytes such as T and B cells (*SI Appendix,* Fig. S2*A*), we further established the CD45$^{-/-}$Rag2$^{-/-}$ mice for excluding the effects of these lymphocytes. First, we identified the ILC2s and ILC progenitors, CHILPs (common helper-like ILC progenitors), by flow cytometry as previously reported (31, 32), and confirmed that the cells in the gate of ILC2s were all CD45 and GATA3 positive (*SI Appendix,* Fig. S2 *B–E*). We found that both ILC2 precursors (ILC2Ps) and KLRG1$^+$ mature ILC2s (mILC2s) increased approximately 2-fold in the bone marrow of CD45$^{-/-}$Rag2$^{-/-}$ mice and CD45$^{-/-}$ mice, whereas CHILPs were unchanged relative to CD45$^{+/+}$Rag2$^{-/-}$ control or

CD45$^{+/+}$ wild-type (WT) mice (Fig. 1 *B* and *C*). Furthermore, the frequency of bone marrow KLRG1$^+$ mILC2s was elevated in CD45$^{-/-}$Rag2$^{-/-}$ mice (Fig. 1*D*). Then, we checked the expression of CCR9, which is a hallmark of ILC2 emigration to intestines (4, 33). The frequency of CCR9$^+$ mature ILC2s increased in the bone marrow of CD45$^{-/-}$Rag2$^{-/-}$ mice, suggesting that migratory behavior in the intestine may be enhanced in CD45$^{-/-}$ ILC2s (*SI Appendix,* Fig. S2*F*). In parallel, the cell number of ILC2s increased in the intestine of CD45$^{-/-}$Rag2$^{-/-}$ mice (*SI Appendix,* Fig. S2*G*), possibly due to the increase of CCR9$^+$ mature ILC2s in the bone marrow. By contrast, we confirmed that the cell numbers of common lymphoid progenitors (CLPs), NK cells, and myeloid cells were unchanged in the bone marrow of CD45$^{-/-}$Rag2$^{-/-}$ mice (*SI Appendix,* Fig. S2*H*). As most ILC2s are tissue-resident, we performed parabiosis experiments to test whether CD45 influences the tissue residency of ILC2s in the bone marrow. WT and CD45$^{-/-}$ ILC2s showed high tissue residency in vivo (*SI Appendix,* Fig. S2*I*). These observations suggest that CD45 limits the expansion and maturation of ILC2s in the bone marrow.

Although we observed an increase of ILC2s in the bone marrow, the cell numbers of ILC2s as well as NK cells and myeloid cells in peripheral tissues such as lung and spleen were comparable between CD45$^{-/-}$Rag2$^{-/-}$ mice and control mice (Fig. 1*E* and *SI Appendix,* Fig. S2*J*). Since ILC2s rapidly express high amounts of type 2 cytokine, such as IL-5 and IL-13, to exert their effector functions (32), we assessed the cytokine production of CD45$^{-/-}$ ILC2s in the lung. The frequencies of IL-5$^+$ and IL-13$^+$ ILC2s from CD45$^{-/-}$Rag2$^{-/-}$ mice were higher than those from control mice after stimulation with PMA and ionomycin (Fig. 1 *F* and *G*). We further performed ex vivo culture of ILC2s from CD45$^{-/-}$Rag2$^{-/-}$ mice or control mice with IL-2 and IL-33, which is the most potent combination of ILC2 activators and is critical for the establishment of allergic inflammation (12, 32). Besides the enhanced frequencies of IL-5$^+$ and IL-13$^+$ ILC2s from CD45$^{-/-}$Rag2$^{-/-}$ mice (Fig. 1 *H* and *I*), the amounts of IL-5 and IL-13 production by CD45$^{-/-}$ ILC2s were also elevated (Fig. 1*J*). Moreover, the cell number of lung CD45$^{-/-}$ ILC2s was higher than CD45$^{+/+}$ ILC2s after 3 d of culture (Fig. 1*K*). On the other hand, both control and CD45$^{-/-}$ ILC2s in the bone marrow showed minimal and equal IL-5 and IL-13 expression levels (*SI Appendix,* Fig. S2*K*). Thus, these results suggest that CD45 suppresses the type 2 cytokine production of lung ILC2s.

Cell-Intrinsic CD45 Signaling Is Required for the Regulation of ILC2s. To determine whether the regulation of ILC2s by CD45 depends on cell-intrinsic CD45 signaling, we generated bone marrow chimera mice (CD45.1 × CD45.2) transferred with a 1:1 mixture of WT (CD45.1) and CD45-deficient (CD45$^{-/-}$) bone marrow cells (Fig. 2*A*). After 8 wk, CD45$^{-/-}$ ILC2s dominated in the bone marrow compared to WT ILC2s (Fig. 2 *B* and *C*). By contrast, CD45-deficient T cells almost disappeared, and the whole T cell population consisted predominantly of WT T cells (Fig. 2 *B* and *C*), consistent with the previous report that CD45 is essential for T cell development (27). Moreover, we found that the frequencies of IL-5$^+$ and IL-13$^+$ cells in CD45$^{-/-}$ ILC2s were higher than in WT ILC2s after stimulation with PMA and ionomycin (Fig. 2 *D* and *E*). Together, these results suggest that cell-intrinsic CD45 signaling enhances the expansion and effector function of ILC2s.

CD45 Modulates Cell Metabolism in ILC2s. Since GATA3 is a crucial transcription factor in ILC2 development, we next examined the GATA3 expression in CD45$^{-/-}$Rag2$^{-/-}$ and control
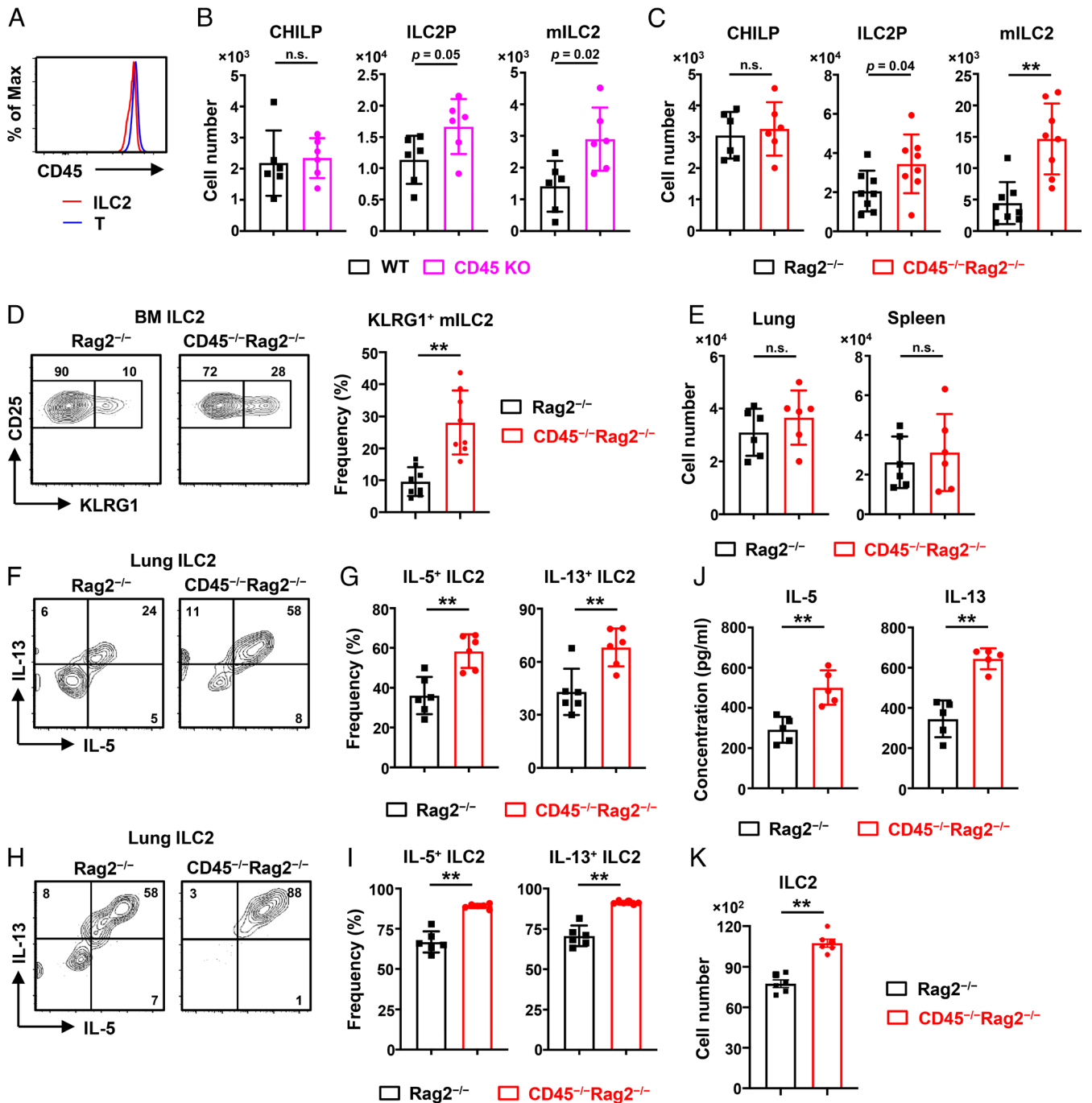
Fig. 1. CD45 restrains expansion, maturation, and cytokine production of ILC2s. ILC2s isolated from CD45 knockout (KO) and wild-type mice (WT) (*A* and *B*) or CD45$^{-/-}$Rag2$^{-/-}$ and control Rag2$^{-/-}$ mice (*C–K*) were analyzed by flow cytometry. (*A*) Expression of CD45 on ILC2s (Lin$^-$IL-7R$^+$Sca-1$^+$CD25$^+$ST2$^+$) and T cells in the bone marrow of WT mice. (*B*) Numbers of common helper-like ILC progenitors (CHILPs) (Lin$^-$IL-7R$^+$CD25$^-$ST2$^-$α4β7$^+$Flt3$^-$), ILC2 precursors (ILC2Ps) (Lin$^-$IL-7R$^+$Sca-1$^+$CD25$^+$ST2$^+$KLRG1$^-$), and mature ILC2s (mILC2s) (Lin$^-$IL-7R$^+$Sca-1$^+$CD25$^+$ST2$^+$KLRG1$^+$) in the bone marrow of CD45 KO and WT mice (n = 6). (*C*) Numbers of CHILPs, ILC2Ps, and mILC2s in the bone marrow of CD45$^{-/-}$Rag2$^{-/-}$ and control mice (n = 6 to 8). (*D*) Flow cytometric analysis and frequency of mILC2s in the bone marrow (n = 8). (*E*) Numbers of ILC2s (Lin$^-$IL-7R$^+$Sca-1$^+$ST2$^+$KLRG1$^+$) in the lung and spleen (n = 6). (*F* and *G*) Flow cytometric analysis (*F*) and frequency (*G*) of IL-5$^+$ and IL-13$^+$ lung ILC2s after stimulation with PMA and ionomycin for 4 h (n = 6). (*H* and *I*) Freshly isolated ILC2s were seeded at 4,000 cells/well in a round bottom 96-well plate and cultured with 10 ng/mL IL-2 and 1 ng/mL IL-33. Flow cytometric analysis (*H*) and frequency (*I*) of IL-5$^+$ and IL-13$^+$ ILC2s after ex vivo culture with IL-2 and IL-33 for 3 d (n = 6). (*J* and *K*) The IL-5 and IL-13 concentrations in the culture supernatants detected by enzyme-linked immunosorbent assay (ELISA) (*J*) and the cell number of ILC2s per well (*K*) after ex vivo culture for 3 d, as shown in *H* and *I* (n = 5 to 6). Data represent at least two independent experiments with similar results (*A*, *D*, *F*, and *H*). Data are mean ± SD with Student's *t* test and pooled from two to four independent experiments (*B–E*, *G*, and *I–K*). **P < 0.01; n.s., not significant.

ILC2s. As we expected, the frequency of GATA3$^+$ST2$^+$ ILC2s was increased in the bone marrow of CD45$^{-/-}$Rag2$^{-/-}$ mice (Fig. 3*A*). In contrast, the GATA3$^+$ST2$^-$ population, which reportedly is circulating ILC2s (34), seemed to decrease in the bone marrow of CD45$^{-/-}$Rag2$^{-/-}$ mice (Fig. 3*A*). However, the levels of GATA3 expression were unchanged between CD45$^{-/-}$Rag2$^{-/-}$ and control

ILC2s in the bone marrow and lung (Fig. 3 *B* and *C*). Thus, these results suggest that GATA3-dependent ILC2 development and activation are not affected by CD45 signaling.

To better understand the effect of CD45 signaling in ILC2s, we compared the gene expression profiles of freshly isolated ILC2s from the bone marrow and lung between CD45$^{-/-}$Rag2$^{-/-}$ and
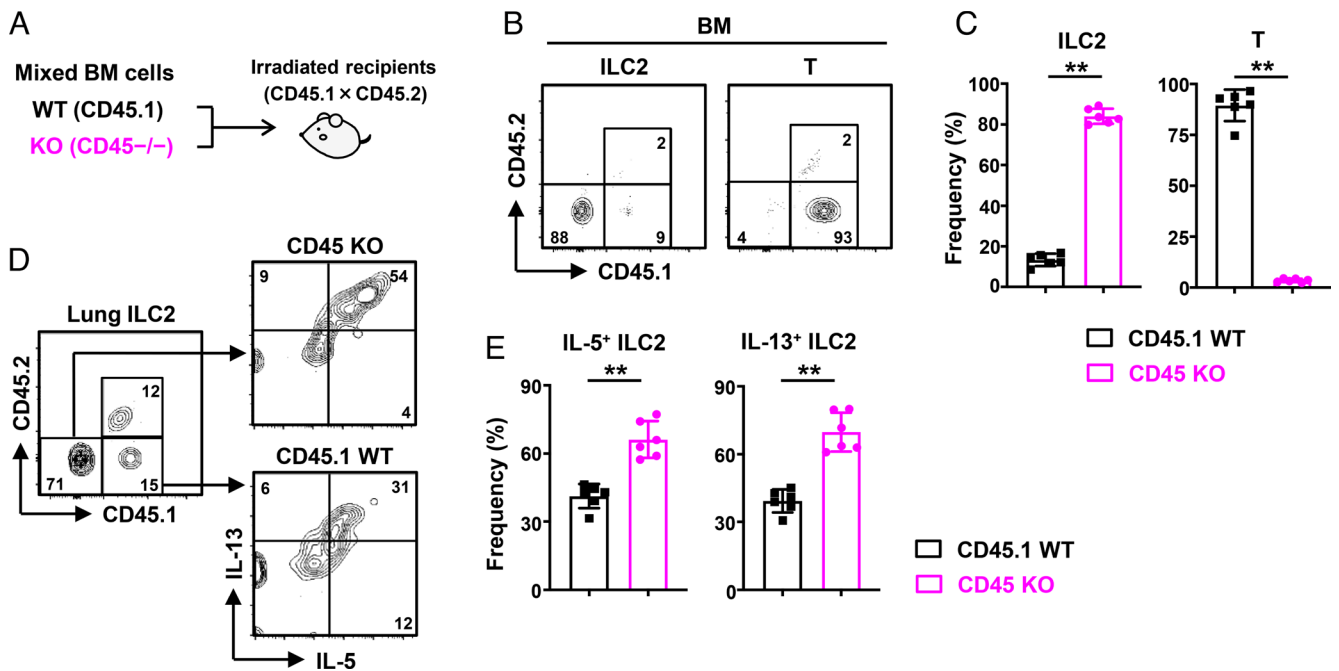
Fig. 2. CD45 regulates ILC2s in a cell-intrinsic manner. (*A*) Lethally irradiated WT mice (CD45.1 × CD45.2) were transferred with a 1:1 mixture of WT (CD45.1) and CD45$^{-/-}$ bone marrow cells and analyzed after 8 wk. (*B* and *C*) Flow cytometric analysis (*B*) and frequency (*C*) of ILC2s and T cells in the bone marrow from the bone marrow chimera mice (n = 6). (*D* and *E*) Flow cytometric analysis (*D*) and frequency (*E*) of IL-5$^+$ and IL-13$^+$ ILC2s isolated from the lung of the bone marrow chimera mice after stimulation with PMA and ionomycin for 4 h (n = 6). Data represent two independent experiments with similar results (*B* and *D*). Data are mean ± SD with Student's *t* test and pooled from two independent experiments (*C* and *E*). **$P < 0.01$.

control mice by digital RNA-seq (dRNA-seq) analysis. The principal component analysis (PCA) showed that CD45 deficiency resulted in similar expression changes in the bone marrow and lung between CD45$^{-/-}$Rag2$^{-/-}$ and control ILC2s, although there was marked heterogeneity of ILC2s between the bone marrow and lung (Fig. 3*D*), which may be due to the high tissue-residency of ILC2s. Enrichment analysis showed that CD45 might regulate the genes involved in cell metabolism, activation, and biological function (Fig. 3*E* and *SI Appendix,* Fig. S3 *A* and *B*). Above all, the three ILC2 populations, CD45$^{-/-}$ ILC2Ps, mILC2s, and lung ILC2s, expressed different levels of genes related to metabolic processes. Moreover, the expression of genes for ribosome biogenesis, related to metabolic activities, was also enhanced in CD45$^{-/-}$ ILC2s (Fig. 3*F*).

To further determine the metabolic changes between control and CD45$^{-/-}$ ILC2s, we employed a metabolic profiling method based on SCENITH (Single Cell Metabolism by Profiling Translation Inhibition) (35) with O-propargyl (OP)-puromycin, which enabled us to assess the metabolic state in low numbers of cells. The method is based on metabolism-dependent translation levels measured by incorporating puromycin into nascent proteins, which is a reliable readout for protein synthesis levels. We cultured lung ILC2s with specific inhibitors, 2-deoxy-D-glucose (DG), oligomycin, or both, and measured the translation levels by incorporating OP-puromycin. We calculated glucose dependence, mitochondrial dependence, glycolytic capacity, and fatty acid and amino acid oxidation (FAAO) capacity by comparing the levels in lung ILC2s. OP-puromycin incorporation was more prominent in CD45$^{-/-}$ ILC2s than in control ILC2s (*SI Appendix,* Fig. S3*C*). We observed a significant increase in glycolytic capacity in CD45$^{-/-}$ ILC2s, whereas control ILC2s had higher mitochondrial dependence (Fig. 3*G*). Then, to confirm the effect of CD45 on glycolysis, we measured glucose incorporation in living lung ILC2s with a fluorescent glucose analog, 2-NBDG, by flow cytometry.

Consistent with the transcriptional analysis and metabolic profiling, CD45$^{-/-}$ ILC2s exhibited elevated glucose uptake (Fig. 3*H*). Taken together, these results indicate that CD45 signaling constantly moderates the metabolism of ILC2s in the steady state and suppresses metabolic shift toward glycolysis.

CD45 Restrains the Proliferation and Survival of ILC2s in the Bone Marrow. The metabolic changes are correlated with cell proliferation, survival, and activation. In accord with the significant increase of ILC2s in CD45$^{-/-}$ and CD45$^{-/-}$Rag2$^{-/-}$ mice (Fig. 1 *B* and *C*), we observed that several genes such as *Pim1*, *Myc*, *Sgk1*, and *Cdc42*, which are involved in cell metabolism, proliferation, and survival, were up-regulated in CD45$^{-/-}$ ILC2Ps of the bone marrow (Fig. 4*A*). In line with the expression of these relevant genes, Ki-67 staining revealed that CD45$^{-/-}$ ILC2s became proliferative in the bone marrow, but not in the lung (Fig. 4*B* and *SI Appendix,* Fig. S3*D*). In addition, the expression of an antiapoptotic factor, Bcl-2, which is vital for cell survival, was moderately elevated in CD45$^{-/-}$ ILC2s of the bone marrow (Fig. 4*C*). These data suggest that CD45 signaling suppresses the proliferation and survival of ILC2s and restrains the population size of ILC2s in the bone marrow in the steady state.

CD45 Restrains Hyperactivation of ILC2s in the Lung. Next, we investigated the activation of CD45$^{-/-}$ ILC2s. Notably, type2 cytokines, including IL-4, IL-5, and IL-13, robustly produced by ILC2s upon activation, were expressed at significantly higher levels in CD45$^{-/-}$ ILC2s compared to control ILC2s from the lung even in the steady state (Fig. 4*D*). The expression of genes related to ILC2 activation, such as *Socs1*, *Ccl1*, *Cxcl2*, *Nfkb1*, *Myc*, *Icos*, *Tnfrsf18* (also known as GITR), and *Selplg* (also known as PSGL-1, P-selectin glycoprotein ligand-1), was enhanced in lung CD45$^{-/-}$ ILC2s in the steady state (Fig. 4*D*), whereas the expression of IL-10 and TIGIT, which are known markers of exhausted ILC2
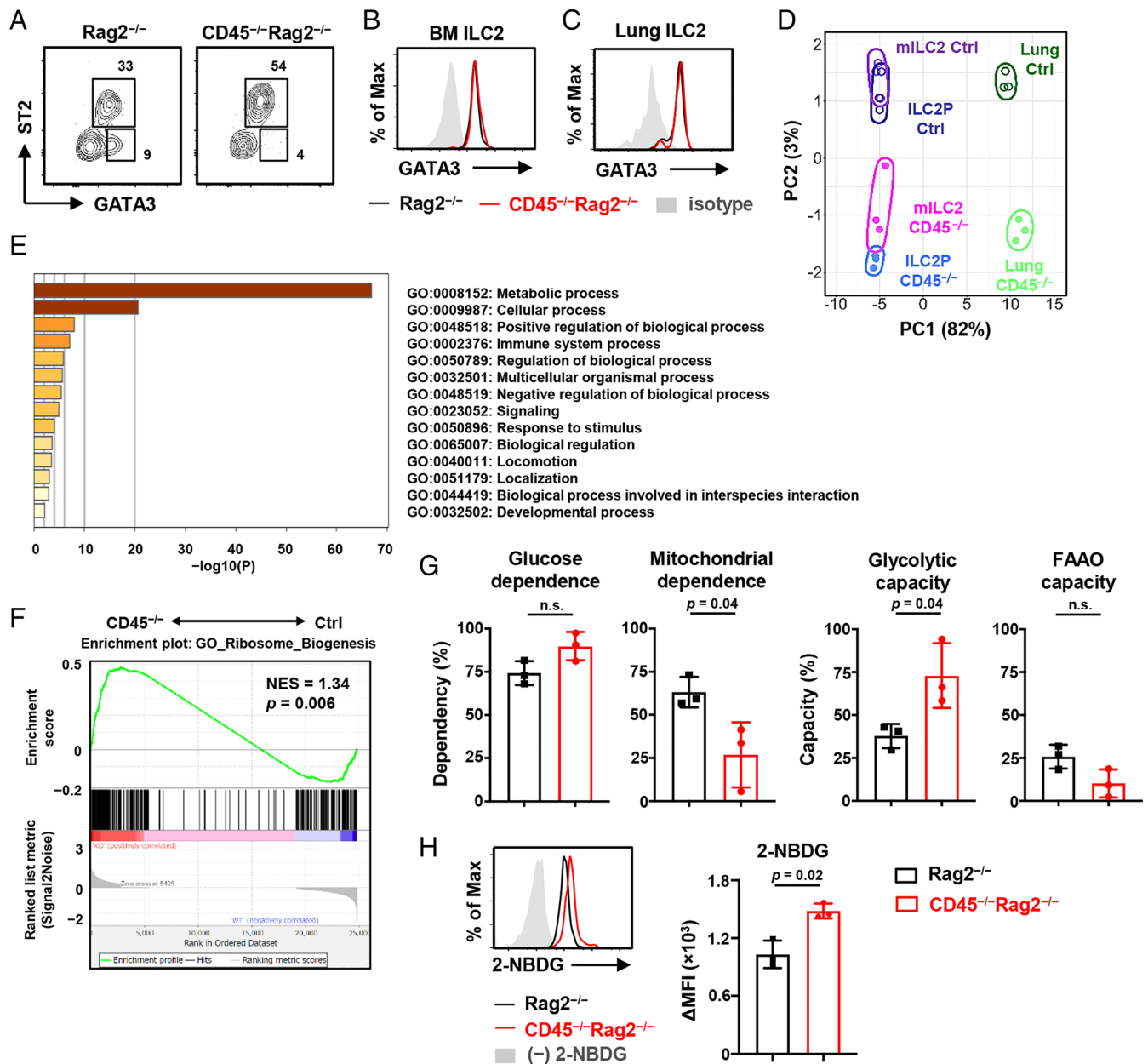
Fig. 3. CD45 limits glycolytic metabolism in ILC2s. ILC2s isolated from CD45$^{-/-}$Rag2$^{-/-}$ and control Rag2$^{-/-}$ mice were analyzed. (*A*) Flow cytometric analysis of Lin$^-$7R$^+$ cells in the bone marrow. (*B* and *C*) Expression levels of GATA3 in bone marrow ILC2s (Lin$^-$IL-7R$^+$Sca-1$^+$CD25$^+$ST2$^+$) (*B*) and lung ILC2s (Lin$^-$IL-7R$^+$CD25$^+$ST2$^+$KLRG1$^+$) (*C*). (*D*) PCA performed among lung ILC2s, bone marrow ILC2Ps, and mILC2s isolated from CD45$^{-/-}$Rag2$^{-/-}$ mice (CD45$^{-/-}$) and Rag2$^{-/-}$ mice (Ctrl). Gene expression data were measured by dRNA-seq from three biological replicates. (*E*) Bar chart depicting the enrichment analysis of differentially expressed genes between lung ILC2s from CD45$^{-/-}$Rag2$^{-/-}$ and Rag2$^{-/-}$ mice. Normalized enrichment scores were calculated using Metascape. (*F*) GSEA of signature genes related to ribosome biogenesis (GO:#0042254) that were differentially expressed in lung CD45$^{-/-}$Rag2$^{-/-}$ ILC2s (CD45$^{-/-}$) compared to control ILC2s (Ctrl). (*G*) Graphs show the percentage of glucose dependence, mitochondrial dependence, glycolytic capacity, and FAAO capacity, calculated using the SCENITH method (n = 3). (*H*) Flow cytometric analysis of 2-NBDG uptake and the corresponding quantification presented as mean fluorescence intensity (MFI) in lung ILC2s (n = 3). Data represent at least two independent experiments with similar results (*A–C*, and *H*). Data are mean ± SD with Student's *t* test and pooled from at least two independent experiments (*G* and *H*). n.s., not significant.

(32), was undetectable in both CD45$^{-/-}$ and control ILC2s by dRNA-seq. Furthermore, the expression of PD-1, induced in IL-33-activated ILC2 (22), was unchanged in CD45$^{-/-}$ ILC2s compared to control ILC2s (*SI Appendix,* Fig. S3E).

Because CD45 is a transmembrane receptor-like protein tyrosine phosphatases and regulates tyrosine phosphorylation of Src family kinases such as Lck, which is essential for T cell development and activation, we then assessed the phosphorylated Lck (p-Lck) levels in ILC2s of CD45$^{-/-}$Rag2$^{-/-}$ and control mice. We found that Lck in CD45$^{-/-}$ ILC2s was hyperphosphorylated on tyrosine residue

Y505 but not Y394 (Fig. 4 *E* and *F*). Furthermore, phosphorylated Fyn (p-Fyn) and Lyn (p-Lyn), the other Src family kinases besides Lck, are also up-regulated in CD45$^{-/-}$ ILC2s compared to control ILC2s (Fig. 4 *G* and *H*). Then, to ask how these Src family kinases relate to the effector function of lung ILC2s, we performed ex vivo culture of ILC2s with or without the Src family kinase inhibitor, PP2 (36). Indeed, both IL-5 and IL-13 expressions by lung ILC2s were down-regulated after adding the Src family kinase inhibitor (Fig. 4 *I* and *J*). Notably, the frequency of IL-5$^+$IL-13$^+$ CD45$^{-/-}$ ILC2s was decreased to a comparable level of CD45$^{+/+}$ ILC2s,
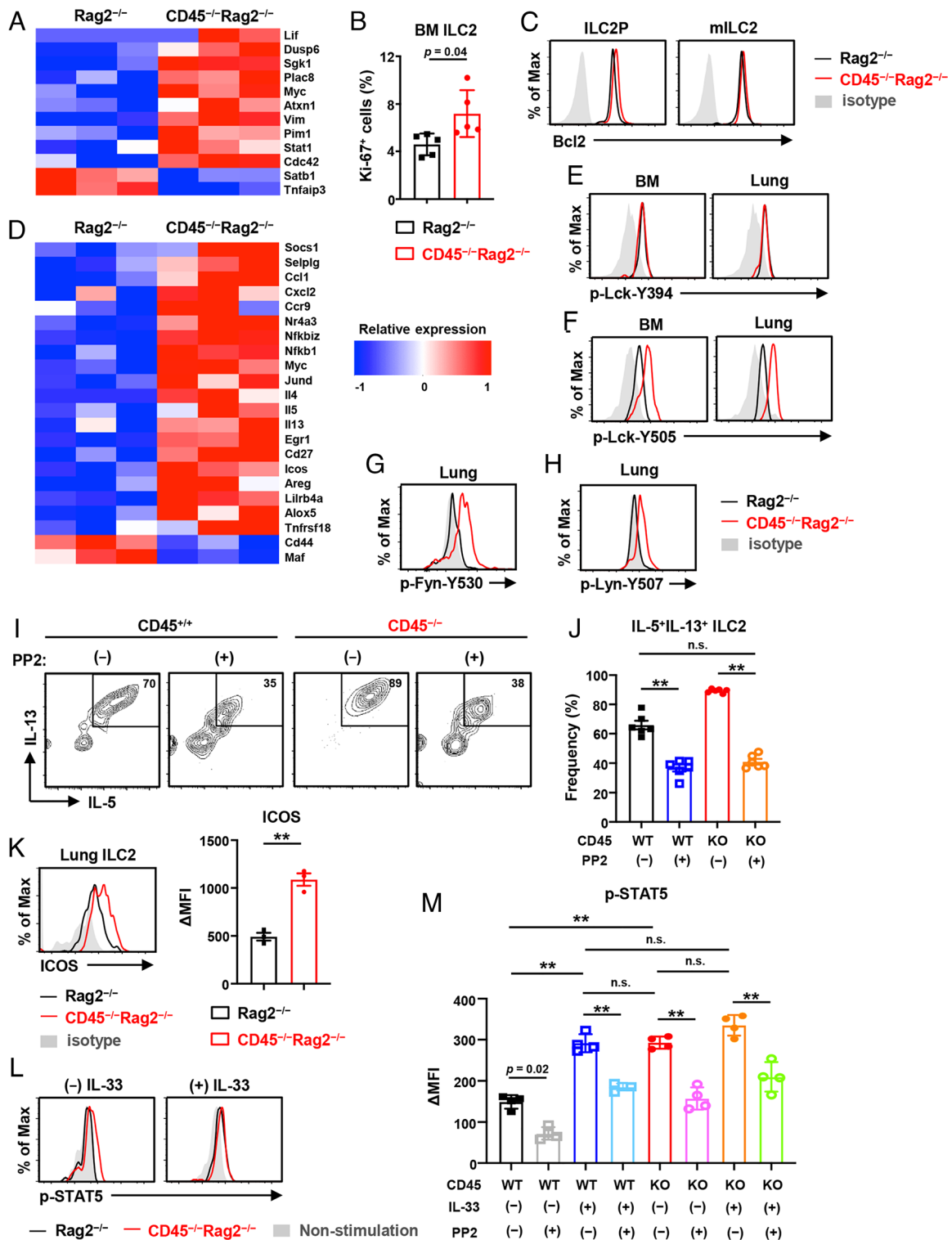
Fig. 4. CD45 restrains proliferation, survival, and hyperactivation of ILC2s. ILC2s isolated from CD45$^{-/-}$Rag2$^{-/-}$ and control Rag2$^{-/-}$ mice were analyzed. (*A*) Heat map of differentially regulated genes involved in cell metabolism, proliferation, and survival of ILC2Ps in the bone marrow with three biological replicates. (*B*) Frequency of proliferating Ki-67$^+$ ILC2s in the bone marrow (n = 5). (*C*) Flow cytometric analysis of Bcl-2 staining of ILC2Ps and mILC2s in the bone marrow. (*D*) Heat map of differentially regulated genes involved in the activation and effector function of ILC2s in the lung with three biological replicates. (*E* and *F*) Flow cytometric analysis of the phosphorylation levels of p-Lck-Y394 (*E*) and p-Lck-Y505 (*F*) in ILC2s from the bone marrow and lung. (*G* and *H*) Flow cytometric analysis of p-Fyn-Y530 (*G*) and p-Lyn-Y507 (*H*) in lung ILC2s. (*I* and *J*) Flow cytometric analysis (*I*) and frequency (*J*) of IL-5$^+$IL-13$^+$ cells in CD45$^{+/+}$ or CD45$^{-/-}$ lung ILC2s after ex vivo culture with 10 ng/mL IL-2 and 1 ng/mL IL-33 and with (+) or without (−) 10 μg/mL PP2, a Src family kinase inhibitor, for 3 d (n = 6). (*K*) Flow cytometric analysis of ICOS expression and the mean fluorescence intensity difference (ΔMFI) between ICOS and isotype control in indicated lung ILC2s (n = 3). (*L*) Flow cytometric analysis for the phosphorylation levels of p-STAT5 in lung ILC2s after stimulation with or without 20 ng/ml IL-33 for 1 d and restimulation with 100 ng/mL IL-2 for 30 min (n = 4). (*M*) ΔMFI between p-STAT5 and isotype control staining in indicated lung ILC2s after stimulation with or without 20 ng/mL IL-33 and with or without 10 μg/mL PP2 for 1 d and after restimulation with 100 ng/mL IL-2 for 30 min (n = 4). Data are mean ± SD with Student's *t* test (*B* and *K*) or one-way ANOVA (*J* and *M*) and pooled from two to three independent experiments. Data represent at least two independent experiments with similar results (*C*, *E–I*, *K*, and *L*). **$P < 0.01$; n.s., not significant.

suggesting that Src family kinases may be involved in the regulation of type 2 cytokine production by CD45.

Furthermore, consistent with the previous report that ICOS-ICOSL signaling is involved in ILC2 effector functions (14), ICOS's mRNA and protein expression levels were constantly elevated in CD45$^{-/-}$ ILC2s (Fig. 4 D and K). Since the signal from ICOS facilitates the type 2 immune response of ILC2s by STAT5 signaling in response to IL-2 and IL-33 (14, 23), we evaluated the levels of phosphorylated STAT5 (p-STAT5) after IL-2 stimulation, which associates with the activation of ILC2s. The levels of p-STAT5 in CD45$^{-/-}$ ILC2s were significantly elevated even by stimulation with IL-2 alone, whereas control ILC2s required both IL-2 and IL-33 for their activation (Fig. 4 L and M). Furthermore, the pSTAT5 levels were decreased in both CD45$^{+/+}$ and CD45$^{-/-}$ ILC2s after PP2 treatment, even with IL-33 stimulation (Fig. 4M). These results suggest that CD45 on lung ILC2s may restrain hyperactivation by regulating Src family kinases and ICOS-ICOSL signaling.

CD45 Signaling Limits Lung Inflammation via ILC2s. ILC2s are a crucial regulator of allergic airway inflammation and pulmonary fibrosis. To address whether CD45 plays a role in regulating the function of lung ILC2s in inflammatory conditions, we first carried out an airway inflammation model with a high dose of papain in CD45$^{-/-}$Rag2$^{-/-}$ mice and control Rag2$^{-/-}$ mice. Since ILC2s reportedly provoke eosinophil infiltration and allergic inflammation in the lung (17, 37), we first analyzed eosinophils in bronchoalveolar lavage (BAL) fluid by flow cytometry (*SI Appendix,* Fig. S4*A*), and the numbers of eosinophils and neutrophils in BAL fluid and ILC2s in the lung of CD45$^{-/-}$Rag2$^{-/-}$ mice were increased compared to those in control mice after intranasal administration of papain for 3 d (Fig. 5 *A* and *B*), whereas eosinophils and neutrophils were very few in BAL fluid and comparable between CD45$^{-/-}$Rag2$^{-/-}$ and control mice in the steady state (*SI Appendix,* Fig. S4 *B* and *C*). Consistent with the increase of ILC2s, the levels of IL-5 and IL-13 production were higher in the BAL fluid of CD45$^{-/-}$Rag2$^{-/-}$ mice than of control mice (Fig. 5*C*). Coincidently, peribronchial infiltration of immune cells was exacerbated in the lung of CD45$^{-/-}$Rag2$^{-/-}$ mice by H&E staining (Fig. 5 *D* and *E*), whereas there was no infiltration of immune cells in CD45$^{-/-}$Rag2$^{-/-}$ and control mice in the steady state (*SI Appendix,* Fig. S4*D*).

Since many leukocytes besides ILC2s also express CD45 and may affect airway inflammation, we performed cell depletion of ILC2s from CD45$^{-/-}$Rag2$^{-/-}$ and Rag2$^{-/-}$ mice with an anti-Thy-1 antibody as described previously (38). We found that the total number of cells in BAL fluid was reduced and the inflammation was alleviated after ILC2 depletion in CD45$^{-/-}$Rag2$^{-/-}$ as well as control mice, suggesting that the exacerbation of inflammation in CD45$^{-/-}$Rag2$^{-/-}$ mice is ILC2-dependent (Fig. 5*F*). To clarify the effects of CD45$^{-/-}$ ILC2s in the papain-induced airway inflammation model, we adoptively transferred CD45$^{-/-}$ ILC2s or control ILC2s into IL-7Rα-deficient recipient mice, which largely lack ILC2s in the lung. The transferred ILC2s were detected in the lung of IL-7Rα-deficient recipient mice, and the number and frequency of IL-5 and IL-13 production were higher in CD45$^{-/-}$ ILC2s than in control ILC2s (Fig. 5 *G* and *H*, and *SI Appendix,* Fig. S4*E*). The number of eosinophils and neutrophils in BAL fluid was significantly increased in mice transferred with CD45$^{-/-}$ ILC2s compared to control ILC2s (Fig. 5*I*). These results suggest that CD45 prevents the pathogenesis of lung inflammation probably by suppressing the population size and activation of ILC2s after stimulation.

CD45 Signaling in ILC2s Limits Lung Fibrosis. ILC2s are involved in pulmonary fibrosis by promoting the activation of myofibroblasts and the deposition of extracellular matrix (19, 20). Notably, we found that amphiregulin (encoded by *Areg*) and Egr1, which are involved in the pathogenesis of fibrosis (25, 39), were highly expressed in lung CD45$^{-/-}$ ILC2s (Fig. 4*D*). In addition, we also observed the high expression of *Areg* in bone marrow mILC2s of CD45$^{-/-}$Rag2$^{-/-}$ mice (*SI Appendix,* Fig. S4*F*). We employed a bleomycin-induced pulmonary fibrosis model to determine whether CD45 influences fibrosis via lung ILC2s. CD45$^{-/-}$Rag2$^{-/-}$ mice exhibited significantly increased collagen deposition in the lung compared with control mice by Masson's trichrome staining (Fig. 5 *J* and *K*), whereas the collagen deposition was hardly detected in the lung of CD45$^{-/-}$Rag2$^{-/-}$ and control Rag2$^{-/-}$ mice in the steady state (*SI Appendix,* Fig. S4*G*). Numbers of neutrophils and macrophages in BAL fluid and ILC2s in lung parenchyma tended to increase in CD45$^{-/-}$Rag2$^{-/-}$ mice 7 d after bleomycin administration (Fig. 5 *L* and *M*). Furthermore, we found that the mortality rate of CD45$^{-/-}$Rag2$^{-/-}$ mice was exacerbated compared to control mice (Fig. 5*N*). These results suggest that CD45 signaling may mitigate the pathogenesis of pulmonary fibrosis, possibly by suppressing ILC2s.

CD45-Galectin-9 Interaction Influences the ILC2 Suppression by CD45. Because previous reports showed that CD45 alters the survival and activation of lymphocytes by binding to galectins such as galectin-1, galectin-3, and galectin-9 (30, 40, 41), we performed ex vivo culture of ILC2s with these galectins. As a result, the production of IL-5 and IL-13 was reduced in control but not CD45$^{-/-}$ ILC2s, when cultured with galectin-9 but not galectin-1 and galectin-3 (Fig. 6*A* and *SI Appendix,* Fig. S5*A*). In addition, we confirmed that galectin-9 was bound to CD45 on the cell surface of control ILC2s (Fig. 6*B*). Since galectin-9 can also interact with CD44, Tim-3, and CD137 (42), we analyzed the expression of these molecules on ILC2s. CD44 was down-regulated in CD45$^{-/-}$ ILC2s, whereas Tim-3 and CD137 were unchanged (Fig. 6*C* and *SI Appendix,* Fig. S5*B*). These results suggest that galectin-9 may suppress the activation of ILC2s through interactions with CD45 and CD44.

To further determine whether galectin-9 has the potential to influence the progression of airway inflammation in vivo, we administrated mice with galectin-9 in the papain-induced airway inflammation model. We found that the numbers of eosinophils in BAL fluid and ILC2s in lung parenchyma were reduced in control Rag2$^{-/-}$ mice by galectin-9 administration (Fig. 6 *D* and *E*). By contrast, the numbers of eosinophils in the BAL fluid were unchanged in CD45$^{-/-}$Rag2$^{-/-}$ mice by galectin-9 administration, whereas ILC2s in lung parenchyma were modestly reduced (Fig. 6 *F* and *G*). In addition, we observed that the peribronchial infiltration of immune cells was alleviated in control Rag2$^{-/-}$ mice treated with galectin-9 (Fig. 6 *H* and *I*) but not in CD45$^{-/-}$Rag2$^{-/-}$ mice (*SI Appendix,* Fig. S5 *C* and *D*). Collectively, these data suggest that the interaction of galectin-9 with CD45 on ILC2s may suppress the cytokine production by ILC2s and possibly contribute to alleviating airway inflammation.

Discussion

In this study, we characterized the roles of CD45 in the development, homeostasis, and effector function of ILC2s. CD45 deficiency enhanced the proliferation, survival, and maturation of ILC2s, leading to the increased population size of ILC2s, especially mILC2s in the bone marrow. CD45$^{-/-}$ ILC2s in the lung exhibited a hyperactivated phenotype, which appeared to reduce the threshold of inflammatory responses. In parallel, CD45$^{-/-}$ ILC2s showed enhanced glycolysis, which provides energy for the proliferation
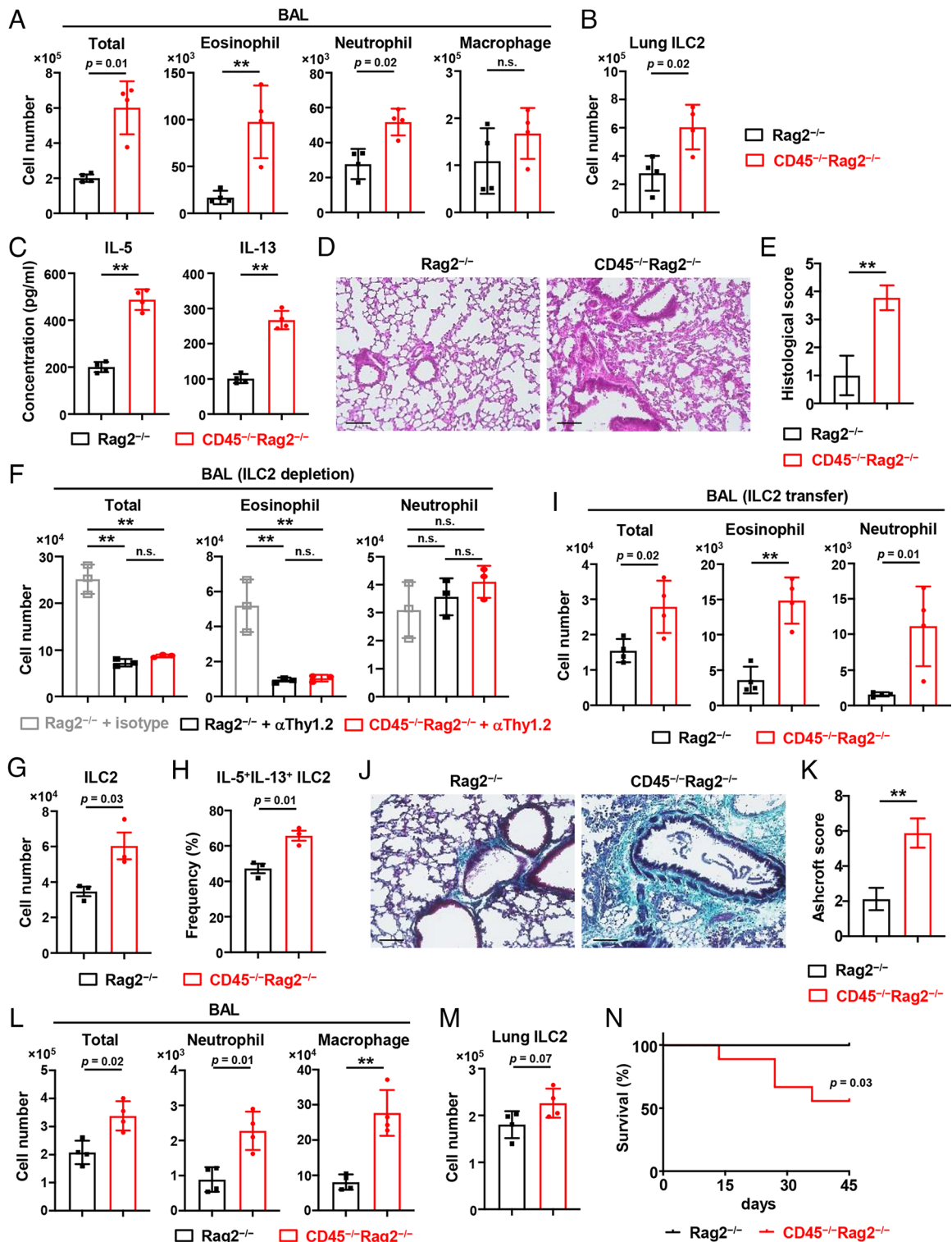
Fig. 5. CD45 limits lung inflammation and fibrosis via ILC2s. (*A* and *B*) CD45$^{-/-}$Rag2$^{-/-}$ and control Rag2$^{-/-}$ mice were intranasally administrated with 50 μg papain daily for 3 consecutive days to induce airway inflammation. Numbers of total cells, eosinophils, neutrophils, and macrophages in BAL fluid (*A*) and ILC2s in the lung (*B*) (n = 4). (*C*) The IL-5 and IL-13 concentrations were detected by ELISA in the BAL fluid from mice, as shown in *A* and *B* (n = 4). (*D* and *E*) H&E staining (*D*) and histological scores (*E*) of the lung from mice, as shown in *A* and *B* (n = 4). (Scale bar, 100 μm.) (*F*) Lung ILC2s in CD45$^{-/-}$Rag2$^{-/-}$ and Rag2$^{-/-}$ mice were depleted by administration with anti-mouse Thy-1.2 (30H12) antibody or control Rag2$^{-/-}$ mice were treated with rat IgG2b isotype control at 2 and 4 d before exposure to papain. After intranasally administrated with papain for 3 consecutive days, total cells, eosinophils, and neutrophils in BAL fluid were measured (n = 3). (*G* and *H*) IL-7Rα KO mice were adoptively transferred with lung ILC2s sorted from CD45$^{-/-}$Rag2$^{-/-}$ or Rag2$^{-/-}$ mice and then intranasally administrated with papain for 3 consecutive days. Numbers of ILC2s (*G*) and frequency of IL-5$^+$IL-13$^+$ ILC2s (*H*) in the lung of IL-7Rα KO recipient mice (n = 3). (*I*) The number of total cells, eosinophils, and neutrophils in the BAL fluid of IL-7Rα KO recipient mice, as shown in *G* and *H* (n = 4). (*J* and *K*) CD45$^{-/-}$Rag2$^{-/-}$ and control Rag2$^{-/-}$ mice were intraperitoneally administrated with 4 mg/kg bleomycin to induce lung fibrosis. Masson's trichrome staining of lung sections (*J*) and Ashcroft scoring of lung fibrosis (*K*) were performed on day 7 (n = 3). (Scale bar, 100 μm.) (*L* and *M*) Numbers of total cells, neutrophils, and macrophages in the BAL fluid (*L*) and ILC2s in the lung (*M*) from mice, as shown in *J* and *K* (n = 4). (*N*) The survival rate of CD45$^{-/-}$Rag2$^{-/-}$ and Rag2$^{-/-}$ mice treated with bleomycin for 45 d. Each group consisted of eight mice, and the log-rank test evaluated the difference. Data are mean ± SD with Student's *t* test (*A–C*, *E*, *I–H*, and *K–M*) or one-way ANOVA (*F*) and pooled from two to three independent experiments. Data represent two independent experiments with similar results (*D*, *J*, and *N*). **$P < 0.01$. n.s., not significant.
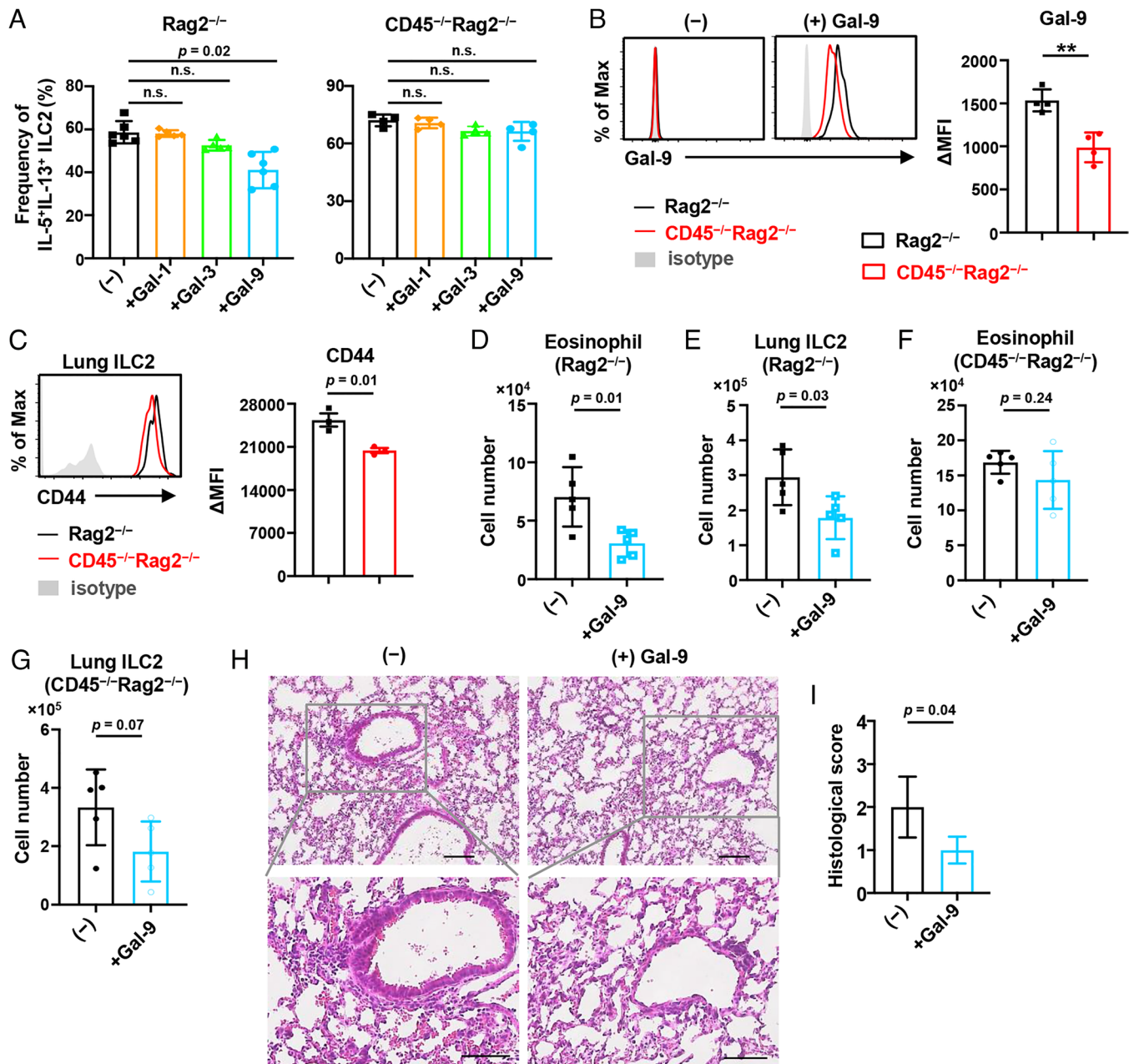
Fig. 6. CD45-galectin-9 interaction influences the ILC2 suppression by CD45. (*A*) Frequency of IL-5⁺IL-13⁺ ILC2s from the lung of CD45⁻/⁻Rag2⁻/⁻ and control Rag2⁻/⁻ mice after ex vivo culture with IL-2, IL-7, IL-33, and with (+) or without (−) 5 µg/mL galectin (Gal)-1, Gal-3, or Gal-9 (n = 4 to 6). (*B*) Flow cytometric analysis of recombinant Gal-9 binding on the lung ILC2s and the mean fluorescence intensity difference (ΔMFI) between CD45⁻/⁻Rag2⁻/⁻ and Rag2⁻/⁻ mice after incubation with 1 µg/mL recombinant mouse Gal-9 for 30 min (n = 4). (*C*) Flow cytometric analysis for the expression of CD44 and ΔMFI between CD44 and isotype control in indicated lung ILC2s (n = 3). (*D–G*) Mice were administered 100 µg papain for 3 consecutive days to induce airway inflammation and with (+Gal-9) or without (−) 30 µg mouse recombinant Gal-9 on the second and third days. Numbers of eosinophils in BAL fluid (*D*) and ILC2s in the lung (*E*) of control Rag2⁻/⁻ mice at day 4 (n = 5). Numbers of eosinophils in the BAL fluid (*F*) and ILC2s in the lung (*G*) of CD45⁻/⁻Rag2⁻/⁻ mice at day 4. (n = 5). (*H* and *I*) H&E staining (*H*) and histological scores (*I*) of the lung from mice as shown in *D* and *E* (n = 4). (Scale bar, 100 µm.) Data represent at least two independent experiments with similar results (*B*, *C*, and *H*). Data are mean ± SD with one-way ANOVA (*A*) or Student's *t* test (*B–G* and *I*) and pooled from two to three independent experiments. **P < 0.01; n.s., not significant.

of T cells and ILC2s. Following the distinct gene expression pattern assessed by dRNA-seq, we found that CD45 affects the bone marrow and lung ILC2s differently, which may be related to the previous observations that ILC2s are distributed into tissues at birth and undergo proliferation and maturation in a tissue-specific manner (34, 43). Moreover, in line with the elevated proliferation and hyperactivated state, inflammation was augmented in the papain-induced airway inflammation model or the mice with adoptive transfer of CD45⁻/⁻ ILC2s. Additionally, pulmonary

fibrosis was exacerbated in bleomycin-treated CD45⁻/⁻Rag2⁻/⁻ mice. Nevertheless, the frequency of GATA3⁺ST2⁻ ILC2s decreased in CD45-deficient mice, suggesting that CD45 may also impact this circulating population of ILC2s (34). However, since we gated ILC2s with ST2 and CD25, which were expressed on tissue-resident ILC2s but not on the circulating population (34, 43), the function of CD45 in circulating ILC2s needs future investigation. Thus, we identified CD45 as a negative regulator in ILC2s in the steady state and inflammation.

Stimulation of ILC2s by IL-33 or IL-25 enhances type 2 immunity and inflammation via NF-κB and AP-1 signaling (44, 45). In the steady state, lung CD45$^{-/-}$ ILC2s expressed higher levels of genes related to type 2 cytokines such as IL-4, IL-5, and IL-13, along with NF-κB and AP-1 signaling like *Nfkb1* and *Jund*. Consistent with the reports that the costimulatory molecule ICOS and GITR were critical for ILC2 activation (14, 15), lung CD45$^{-/-}$ ILC2s highly expressed these molecules. Recent reports showed that Myc plays a critical role in the proliferation and cytokine production of ILC2s, and the *Myc* expression is increased in ILC2s of asthma patients (46). Since *Myc* expression was up-regulated in CD45$^{-/-}$ ILC2s, the elevation of proliferation and cytokine production in lung CD45$^{-/-}$ ILC2s may be in part due to the regulation by Myc. Furthermore, CD45$^{-/-}$ ILC2s expressed higher levels of SOCS1 compared to control ILC2s in the lung, suggesting that CD45 may up-regulate SOCS1 to inhibit interferon and STAT1 signals, which reportedly regulate ILC2s negatively (21, 47). However, the expressions of IL-10 and TIGIT were not enhanced in CD45$^{-/-}$ ILC2s, suggesting that CD45$^{-/-}$ ILC2s are in a state different from the condition of exhausted ILC2. Taken together, lung CD45$^{-/-}$ ILC2s exhibit hyperactivation phenotypes in the steady state with the massive expression of genes related to activation.

Since CD45 is a transmembrane tyrosine phosphatase controlling the Src family kinase activity such as Lck, Fyn, and Lyn (28, 29), the higher level of p-Lck Y505, p-Fyn, and p-Lyn in CD45$^{-/-}$ ILC2s suggests that the dephosphorylation of these Src family kinases is involved in regulating ILC2 activation by CD45. Recently, ICOS reportedly associates with Lck and mediates PI3K activation (48), suggesting that CD45 may control the ICOS-mediated PI3K signaling pathway associated with Lck regulation in ILC2s.

ILC2s and Th2 cells share many transcription factors or costimulatory molecules with similar functions. The transcription factors, including TCF-1, RORα, Gfi1, and GATA3, are important for their development or type 2 immune response (4–7). In addition, the costimulatory molecules like ICOS and GITR positively, whereas PD-1 negatively, regulate their activation (14, 15, 22). Here, we demonstrated that CD45 is another critical regulator for T cells and ILC2s. Of note, CD45 positively controls T cell development but negatively regulates the expansion, maturation, and activation of ILC2s differently from the factors that exert similar functions shared between T cells and ILC2s. Therefore, this study suggests that CD45 signaling may balance adaptive and innate immunity by exerting the opposite effects on T cells and ILC2s.

A rapid increase in glycolysis is an early event during T cell activation required for subsequent proliferation, differentiation, and functions of T cells (49). In addition to glycolysis, ILC2s appear to depend on fatty acid metabolisms (50). However, we observed that the metabolism in ILC2s shifted toward the glycolysis in CD45$^{-/-}$ ILC2s. Furthermore, CD45$^{-/-}$ ILC2s exhibited elevated glucose uptake. Thus, the enhanced proliferation and activation of CD45$^{-/-}$ ILC2s may be due to the alteration of glycolytic metabolism, similar to a previous report on PD-1-deficient ILC2s (22). Notably, the transcription factor Myc, which controls the metabolic reprogramming upon T cell activation (51), was up-regulated in CD45$^{-/-}$ ILC2s. In addition, *Sgk1* expression was elevated in CD45$^{-/-}$ ILC2s, consistent with a recent report that Sgk1 is involved in glucose metabolism (52). Moreover, CD45 signaling modulates ribosome biogenesis in ILC2s, which drives metabolic reprogramming, proliferation, and differentiation during T cell activation (53). CD45 may limit the proliferation and activation of ILC2s in the steady state by repressing glycolysis through Myc, Sgk1, and ribosome biogenesis.

Previous reports showed that the frequency and activity of ILC2s are elevated in patients with asthma and idiopathic pulmonary fibrosis (18, 19). The papain-induced airway inflammation was exacerbated in CD45-deficient mice or by adoptive transfer of CD45$^{-/-}$ ILC2s, whereas it was alleviated by ILC2 depletion, suggesting that CD45 on ILC2 plays an essential role in the suppression of airway inflammation. Since most ILC2s are tissue-resident and maintained by self-renewal in the peripheral tissues (34, 43), the elevated expansion and activation of lung ILC2s in CD45$^{-/-}$ mice during inflammation may be due to the hyperactivation of CD45$^{-/-}$ ILC2s within the lung. Alternatively, the increased mature ILC2s in the bone marrow of CD45-deficient mice might accelerate their migration into peripheral tissues under inflammation. Functionally, besides the type 2 cytokines, IL-5 and IL-13, and the costimulatory molecules, ICOS and GITR, CD45$^{-/-}$ ILC2s highly expressed Ccl1 and Cxcl2, which are essential for the recruitment of eosinophils and neutrophils (54, 55). Furthermore, amphiregulin, induced by IL-33 and associated with fibrosis, is highly expressed in activated ILC2s (39). Additionally, Egr1 is required for connective tissue remodeling, and Egr1-deficient mice are protected from fibrosis (25). Since CD45$^{-/-}$ ILC2s expressed amphiregulin and Egr1 at high levels, CD45 may prevent the exacerbation of lung inflammation and fibrosis also by limiting the expression of the chemokines and amphiregulin, besides the expression of type 2 cytokines and costimulatory molecules. However, as CD45 is expressed on all hematopoietic cells, the possible effects outside of ILC2s related to exacerbating airway inflammation and lung fibrosis in CD45$^{-/-}$Rag2$^{-/-}$ mice need further investigation.

Galectins are a family of β-galactoside-binding lectins with functions in various biological processes such as cell chemoattraction, activation, and apoptosis. In asthma patients, the productions of galectin-1 and galectin-9 by leukocytes in sputum samples are significantly reduced, in parallel with the increase of type 2 cytokines such as IL-5 and IL-13 (56). Galectin-9 reportedly inhibits allergic airway inflammation in the mouse model (42). Although many galectins reportedly bind to lymphocytes such as T and B cells, galectin-9, not galectin-1 and galectin-3, affected ILC2s. This specificity may be due to the different types of galectins and distinct mechanisms of cell surface molecule clustering by each galectin (30, 57, 58). This study provided a possible explanation for this phenomenon that galectin-9 interacts with CD45 on ILC2s to modulate CD45 clustering and phosphatase activity, which alters the ILC2 suppression by CD45 signaling and limits airway inflammation. However, since galectin-9 is a vital chemoattractant for eosinophils and neutrophils, which express CD45 and are associated with allergic inflammation in asthma (59), galectin-9 may affect the number and activation of eosinophils and neutrophils in an ILC2-independent manner. Furthermore, galectin-9 binds to CD44 and induces apoptosis of activated T cells by inhibiting the CD44-hyaluronan interaction (42). Therefore, the reduction of CD45$^{-/-}$ ILC2s in papain-induced airway inflammation by galectin-9 may be due to the galectin-9-CD44 interaction in ILC2s like in T cells and the influence by eosinophils and neutrophils. Thus, ILC2s may also be involved in the galectin-9-mediated attenuation of allergic airway inflammation via the suppression of type 2 cytokine production by CD45 signaling.

This study identifies CD45 as a unique regulator of development and activation of ILC2s in the steady state, preventing excessive type 2 inflammation and fibrosis in the lung. Our findings highlight that CD45 is an unidentified regulator of pulmonary inflammation and fibrosis via ILC2s, proposing CD45 as a potential therapeutic target to control asthma and pulmonary fibrosis.

Materials and Methods

A detailed description of cell culture, flow cytometry and antibodies, mixed bone marrow chimera, real-time RT-PCR, and parabiosis is provided in *SI Appendix, Materials and Methods*.

Mice. CD45-deficient mice, spontaneously arising in our C57BL/6 mouse colony, carried a deletion of the exon 14 in the CD45 locus as shown in *SI Appendix, Fig. S1*. Rag2-deficient (60), IL-7Rα-deficient (61), and CD45.1 or CD45.2 congenic mice on a C57BL/6 background were used. Additional information is provided in *SI Appendix, Materials and Methods*.

Cell Isolation. Cells were isolated as described (11, 62) and detailed in *SI Appendix, Materials and Methods*.

Digital RNA-seq and Data Analysis. Digital RNA-sequencing (dRNA-seq) was performed as described previously (63–65). Differential gene expression and PCA were performed using rlog-normalized dRNA-seq data by DESeq2 (66). Gene set enrichment analysis (GSEA) (Broad Institute) and enrichment analysis using Metascape (67) were performed. Additional information is provided in *SI Appendix, Materials and Methods*.

Adoptive Transfer of ILC2s. As previously reported, an adoptive transfer experiment using IL-7Rα-deficient mice was performed (12), as detailed in *SI Appendix, Materials and Methods*.

Papain-Induced Pulmonary Inflammation. Papain was intranasally administrated into the recipient mice. ILC2 depletion was performed as previously reported (38). Lung injury was scored as previously described (32). A detailed description is provided in *SI Appendix, Materials and Methods*.

Bleomycin-Induced Pulmonary Fibrosis. Mice were intraperitoneally (i.p.) injected with bleomycin. The Ashcroft score for lung fibrosis was described previously (19, 68). A detailed description is provided in *SI Appendix, Materials and Methods*.

Galectin Staining by Flow Cytometry. A galectin staining experiment was performed, as previously reported (41), detailed in *SI Appendix, Materials and Methods*.

Metabolic Profiling by the Modified SCENITH Method with OP-Puromycin. The flow cytometry–based metabolic profiling was performed by the SCENITH method as described (35), with modifications by using the Click-iT Plus OPP Alexa Fluor 488 Protein Synthesis Assay Kit (Thermo Fisher Scientific). A detailed description is provided in *SI Appendix, Materials and Methods*.

Statistical Analysis. All statistical analyses were performed using GraphPad Prism 7 or 8 software, as detailed in *SI Appendix, Materials and Methods*.

Data and Materials Availability. The gene expression data of dRNA-seq were deposited into the Gene Expression Omnibus (GEO) public dataset with accession number GSE212115 (https://www.ncbi.nlm.nih.gov/geo/query/acc.cgi?acc= GSE212115) (69). All other data are included in the manuscript and/or *SI Appendix*.

Author affiliations: [a]Laboratory of Immune Regulation, Department of Virus Research, Institute for Life and Medical Sciences, Kyoto University, Kyoto 606-8507, Japan; [b]Department of Human Health Sciences, Graduate School of Medicine, Kyoto University, Kyoto 606-8501, Japan; [c]Laboratory for Prediction of Cell Systems Dynamics, RIKEN Center for Biosystems Dynamics Research, Osaka 565-0874, Japan; [d]Center for Genomic Medicine, Graduate School of Medicine, Kyoto University, Kyoto 606-8501, Japan; and [e]Department of Medical Biology, Graduate School of Medicine, Akita University, Akita 010-8543, Japan

1. C. S. Klose, D. Artis, Innate lymphoid cells as regulators of immunity, inflammation and tissue homeostasis. *Nat. Immunol.* **17**, 765–774 (2016).
2. K. Moro *et al.*, Innate production of T_H2 cytokines by adipose tissue-associated c-Kit+Sca-1+ lymphoid cells. *Nature* **463**, 540–544 (2010).
3. R. R. Ricardo-Gonzalez *et al.*, Tissue signals imprint ILC2 identity with anticipatory function. *Nat. Immunol.* **19**, 1093–1099 (2018).
4. T. Hoyler *et al.*, The transcription factor GATA-3 controls cell fate and maintenance of type 2 innate lymphoid cells. *Immunity* **37**, 634–648 (2012).
5. Q. Yang *et al.*, T cell factor 1 is required for group 2 innate lymphoid cell generation. *Immunity* **38**, 694–704 (2013).
6. T. Y. Halim *et al.*, Retinoic-acid-receptor-related orphan nuclear receptor alpha is required for natural helper cell development and allergic inflammation. *Immunity* **37**, 463–474 (2012).
7. C. J. Spooner *et al.*, Specification of type 2 innate lymphocytes by the transcriptional determinant Gfi1. *Nat. Immunol.* **14**, 1229–1236 (2013).
8. N. Serafini, C. A. Vosshenrich, J. P. Di Santo, Transcriptional regulation of innate lymphoid cell fate. *Nat. Rev. Immunol.* **15**, 415–428 (2015).
9. Y. Huang *et al.*, S1P-dependent interorgan trafficking of group 2 innate lymphoid cells supports host defense. *Science* **359**, 114–119 (2018).
10. Y. Huang *et al.*, IL-25-responsive, lineage-negative KLRG1hi cells are multipotential "inflammatory" type 2 innate lymphoid cells. *Nat. Immunol.* **16**, 161–169 (2015).
11. G. Cui *et al.*, IL-7R-dependent phosphatidylinositol 3-kinase competes with the STAT5 signal to modulate T cell development and homeostasis. *J. Immunol.* **204**, 844–857 (2020).
12. K. R. Bartemes *et al.*, IL-33-responsive lineage⁻CD25+CD44hi lymphoid cells mediate innate type 2 immunity and allergic inflammation in the lungs. *J. Immunol.* **188**, 1503–1513 (2012).
13. T. Y. Halim, R. H. Krauss, A. C. Sun, F. Takei, Lung natural helper cells are a critical source of Th2 cell-type cytokines in protease allergen-induced airway inflammation. *Immunity* **36**, 451–463 (2012).
14. H. Maazi *et al.*, ICOS:ICOS-ligand interaction is required for type 2 innate lymphoid cell function, homeostasis, and induction of airway hyperreactivity. *Immunity* **42**, 538–551 (2015).
15. L. Galle-Treger *et al.*, Costimulation of type-2 innate lymphoid cells by GITR promotes effector function and ameliorates type 2 diabetes. *Nat. Commun.* **10**, 713 (2019).
16. B. P. Hurrell *et al.*, TNFR2 signaling enhances ILC2 survival, function, and induction of airway hyperreactivity. *Cell Rep.* **29**, 4509–4524 (2019).
17. R. G. Klein Wolterink *et al.*, Pulmonary innate lymphoid cells are major producers of IL-5 and IL-13 in murine models of allergic asthma. *Eur. J. Immunol.* **42**, 1106–1116 (2012).
18. S. G. Smith *et al.*, Increased numbers of activated group 2 innate lymphoid cells in the airways of patients with severe asthma and persistent airway eosinophilia. *J. Allergy Clin. Immunol.* **137**, 75–86 (2016).
19. E. Hams *et al.*, IL-25 and type 2 innate lymphoid cells induce pulmonary fibrosis. *Proc. Natl. Acad. Sci. U.S.A.* **111**, 367–372 (2014).
20. D. Li *et al.*, IL-33 promotes ST2-dependent lung fibrosis by the induction of alternatively activated macrophages and innate lymphoid cells in mice. *J. Allergy Clin. Immunol.* **134**, 1422–1432 (2014).
21. K. Moro *et al.*, Interferon and IL-27 antagonize the function of group 2 innate lymphoid cells and type 2 immune responses. *Nat. Immunol.* **17**, 76–86 (2016).
22. D. G. Helou *et al.*, PD-1 pathway regulates ILC2 metabolism and PD-1 agonist treatment ameliorates airway hyperreactivity. *Nat. Commun.* **11**, 3998 (2020).
23. S. Taylor *et al.*, PD-1 regulates KLRG1+ group 2 innate lymphoid cells. *J. Exp. Med.* **214**, 1663–1678 (2017).
24. S. Li *et al.*, Aryl hydrocarbon receptor signaling cell intrinsically inhibits intestinal group 2 innate lymphoid cell function. *Immunity* **49**, 915–928 (2018).
25. Y. Nakatsuka *et al.*, Profibrotic function of pulmonary group 2 innate lymphoid cells is controlled by regnase-1. *Eur. Respir. J.* **57**, 2000018 (2021).
26. K. Kishihara *et al.*, Normal B lymphocyte development but impaired T cell maturation in CD45-exon6 protein tyrosine phosphatase-deficient mice. *Cell* **74**, 143–156 (1993).
27. K. F. Byth *et al.*, CD45-null transgenic mice reveal a positive regulatory role for CD45 in early thymocyte development, in the selection of CD4+CD8+ thymocytes, and B cell maturation. *J. Exp. Med.* **183**, 1707–1718 (1996).
28. L. McNeill *et al.*, The differential regulation of Lck kinase phosphorylation sites by CD45 is critical for T cell receptor signaling responses. *Immunity* **27**, 425–437 (2007).
29. P. Shrivastava, T. Katagiri, M. Ogimoto, K. Mizuno, H. Yakura, Dynamic regulation of Src-family kinases by CD45 in B cells. *Blood* **103**, 1425–1432 (2004).
30. J. T. Nguyen *et al.*, CD45 modulates galectin-1-induced T cell death: Regulation by expression of core 2 O-glycans. *J. Immunol.* **167**, 5697–5707 (2001).
31. A. H. Lei *et al.*, ICAM-1 controls development and function of ILC2. *J. Exp. Med.* **215**, 2157–2174 (2018).
32. C. Miyamoto *et al.*, Runx/Cbfβ complexes protect group 2 innate lymphoid cells from exhausted-like hyporesponsiveness during airway inflammation. *Nat. Commun.* **10**, 447 (2019).
33. M. H. Kim, E. J. Taparowsky, C. H. Kim, Retinoic acid differentially regulates the migration of innate lymphoid cell subsets to the gut. *Immunity* **43**, 107–119 (2015).
34. R. R. Ricardo-Gonzalez *et al.*, Tissue-specific pathways extrude activated ILC2s to disseminate type 2 immunity. *J. Exp. Med.* **217** (2020).
35. R. J. Arguello *et al.*, SCENITH: A flow cytometry-based method to functionally profile energy metabolism with single-cell resolution. *Cell Metab.* **32**, 1063–1075 (2020).
36. A. M. Nyakeriga, H. Garg, A. Joshi, TCR-induced T cell activation leads to simultaneous phosphorylation at Y505 and Y394 of p56lck residues. *Cytometry A* **81**, 797–805 (2012).
37. M. Kubo, Innate and adaptive type 2 immunity in lung allergic inflammation. *Immunol. Rev.* **278**, 162–172 (2017).
38. J. W. Krempski, T. Kobayashi, K. Iijima, A. N. McKenzie, H. Kita, Group 2 innate lymphoid cells promote development of T follicular helper cells and initiate allergic sensitization to peanuts. *J. Immunol.* **204**, 3086–3096 (2020).
39. L. A. Monticelli *et al.*, IL-33 promotes an innate immune pathway of intestinal tissue protection dependent on amphiregulin-EGFR interactions. *Proc. Natl. Acad. Sci. U.S.A.* **112**, 10762–10767 (2015).

40. B. N. Stillman et al., Galectin-3 and galectin-1 bind distinct cell surface glycoprotein receptors to induce T cell death. *J. Immunol.* **176**, 778–789 (2006).
41. N. Giovannone et al., Galectin-9 suppresses B cell receptor signaling and is regulated by I-branching of N-glycans. *Nat. Commun.* **9**, 3287 (2018).
42. S. Katoh et al., Galectin-9 inhibits CD44-hyaluronan interaction and suppresses a murine model of allergic asthma. *Am. J. Respir. Crit. Care Med.* **176**, 27–35 (2007).
43. C. Schneider et al., Tissue-resident group 2 innate lymphoid cells differentiate by layered ontogeny and in situ perinatal priming. *Immunity* **50**, 1425–1438 (2019).
44. L. Wang et al., Adiponectin restrains ILC2 activation by AMPK-mediated feedback inhibition of IL-33 signaling. *J. Exp. Med.* **218**, e20191054 (2021).
45. M. Verma et al., The molecular and epigenetic mechanisms of innate lymphoid cell (ILC) memory and its relevance for asthma. *J. Exp. Med.* **218**, e20201354 (2021).
46. L. Ye et al., A critical role for c-Myc in group 2 innate lymphoid cell activation. *Allergy* **75**, 841–852 (2020).
47. X. Dai et al., SOCS1-negative feedback of STAT1 activation is a key pathway in the dsRNA-induced innate immune response of human keratinocytes. *J. Invest. Dermatol.* **126**, 1574–1581 (2006).
48. Z. Wan et al., Transmembrane domain-mediated Lck association underlies bystander and costimulatory ICOS signaling. *Cell Mol. Immunol.* **17**, 143–152 (2020).
49. A. V. Menk et al., Early TCR signaling induces rapid aerobic glycolysis enabling distinct acute T cell effector functions. *Cell Rep.* **22**, 1509–1521 (2018).
50. C. Wilhelm et al., Critical role of fatty acid metabolism in ILC2-mediated barrier protection during malnutrition and helminth infection. *J. Exp. Med.* **213**, 1409–1418 (2016).
51. R. Wang et al., The transcription factor Myc controls metabolic reprogramming upon T lymphocyte activation. *Immunity* **35**, 871–882 (2011).
52. J. A. Mason et al., SGK1 signaling promotes glucose metabolism and survival in extracellular matrix detached cells. *Cell Rep.* **34**, 108821 (2021).
53. A. Galloway et al., Upregulation of RNA cap methyltransferase RNMT drives ribosome biogenesis during T cell activation. *Nucleic Acids Res.* **49**, 6722–6738 (2021).
54. B. Bishop, C. M. Lloyd, CC chemokine ligand 1 promotes recruitment of eosinophils but not Th2 cells during the development of allergic airways disease. *J. Immunol.* **170**, 4810–4817 (2003).
55. G. Wang et al., Macrophagic extracellular vesicle CXCL2 recruits and activates the neutrophil CXCR2/PKC/NOX4 axis in sepsis. *J. Immunol.* **207**, 2118–2128 (2021).
56. S. Sanchez-Cuellar et al., Reduced expression of galectin-1 and galectin-9 by leucocytes in asthma patients. *Clin. Exp. Immunol.* **170**, 365–374 (2012).
57. F. T. Liu, S. R. Stowell, The role of galectins in immunity and infection. *Nat. Rev. Immunol.* **23**, 479–494 (2023).
58. G. Furlan, T. Minowa, N. Hanagata, C. Kataoka-Hamai, Y. Kaizuka, Phosphatase CD45 both positively and negatively regulates T cell receptor phosphorylation in reconstituted membrane protein clusters. *J. Biol. Chem.* **289**, 28514–28525 (2014).
59. R. Matsumoto et al., Human ecalectin, a variant of human galectin-9, is a novel eosinophil chemoattractant produced by T lymphocytes. *J. Biol. Chem.* **273**, 16976–16984 (1998).
60. Y. Shinkai et al., RAG-2-deficient mice lack mature lymphocytes owing to inability to initiate V(D)J rearrangement. *Cell* **68**, 855–867 (1992).
61. K. Maki et al., Interleukin 7 receptor-deficient mice lack gammadelta T cells. *Proc. Natl. Acad. Sci. U.S.A.* **93**, 7172–7177 (1996).
62. Y. Zhu et al., Intestinal epithelial cell-derived IL-15 determines local maintenance and maturation of intra-epithelial lymphocytes in the intestine. *Int. Immunol.* **32**, 307–319 (2020).
63. K. Shiroguchi, T. Z. Jia, P. A. Sims, X. S. Xie, Digital RNA sequencing minimizes sequence-dependent bias and amplification noise with optimized single-molecule barcodes. *Proc. Natl. Acad. Sci. U.S.A.* **109**, 1347–1352 (2012).
64. T. Ogawa, K. Kryukov, T. Imanishi, K. Shiroguchi, The efficacy and further functional advantages of random-base molecular barcodes for absolute and digital quantification of nucleic acid molecules. *Sci. Rep.* **7**, 13576 (2017).
65. G. Cui et al., A circulating subset of iNKT cells mediates antitumor and antiviral immunity. *Sci. Immunol.* **7**, eabj8760 (2022).
66. M. I. Love, W. Huber, S. Anders, Moderated estimation of fold change and dispersion for RNA-seq data with DESeq2. *Genome Biol.* **15**, 550 (2014).
67. Y. Y. Zhou et al., Metascape provides a biologist-oriented resource for the analysis of systems-level datasets. *Nat. Commun.* **10**, 1523 (2019).
68. J. Lv et al., BLT1 mediates bleomycin-induced lung fibrosis independently of neutrophils and CD4^{+} T cells. *J. Immunol.* **198**, 1673–1684 (2017).
69. G. Cui, Z. Jin, N. Hojo, K. Shiroguchi, K. Ikuta, Gene expression profiling of bone marrow and lung ILC2s. Gene Expression Omnibus (GEO). https://www.ncbi.nlm.nih.gov/geo/query/acc.cgi?acc=GSE212115. Accessed 26 August 2022.